



HAL
open science

Comparative study of the high-temperature auto-ignition of cyclopentane and tetrahydrofuran

Hong-quan Do, Benoîte Lefort, Zeynep Serinyel, Luis Le Moyne, Guillaume Dayma

► **To cite this version:**

Hong-quan Do, Benoîte Lefort, Zeynep Serinyel, Luis Le Moyne, Guillaume Dayma. Comparative study of the high-temperature auto-ignition of cyclopentane and tetrahydrofuran. *International Journal of Chemical Kinetics*, 2023, 56 (4), pp.199-209. 10.1002/kin.21703 . hal-04360299

HAL Id: hal-04360299

<https://cnrs.hal.science/hal-04360299v1>

Submitted on 18 Dec 2024

HAL is a multi-disciplinary open access archive for the deposit and dissemination of scientific research documents, whether they are published or not. The documents may come from teaching and research institutions in France or abroad, or from public or private research centers.

L'archive ouverte pluridisciplinaire **HAL**, est destinée au dépôt et à la diffusion de documents scientifiques de niveau recherche, publiés ou non, émanant des établissements d'enseignement et de recherche français ou étrangers, des laboratoires publics ou privés.



Distributed under a Creative Commons Attribution 4.0 International License

1 **Comparative study of the high-temperature auto-ignition**
2 **of cyclopentane and tetrahydrofuran**

3
4 Hong-Quan Do^{a,b}, Benoîte Lefort^{a*}, Zeynep Serinyel^{b,c}, Luis LeMoyne^a and
5 Guillaume Dayma^{b,c*}

6 ^a *DRIVE, Université de Bourgogne-Franche Comté, 49 rue Mademoiselle Bourgeois,*
7 *58000 Nevers, France*

8
9 ^b *Université d'Orléans, 6 Avenue du Parc Floral, 45100 Orléans, France*

10
11 ^c *ICARE-CNRS, 1C, Avenue de la recherche scientifique, 45071 Orléans cedex 2,*
12 *France*

13
14 **Full-Length Article**

15
16
17 * Corresponding authors:

18 Pr. Benoîte Lefort

19 Email: benoite.lefort@u-bourgogne.fr

20 Pr. Guillaume Dayma

21 Email: guillaume.dayma@cnrs-orleans.fr

24 **Abstract:**

25 Cyclopentane (C₅H₁₀) and tetrahydrofuran (C₄H₈O) are both 5-membered ring compounds.

26 The present study compares the auto-ignition of cyclopentane and tetrahydrofuran in a high-

27 pressure shock-tube (20 atm). 12 different mixtures were investigated at two different fuel

28 initial mole fractions (1% and 2%): at $X_{\text{fuel}} = 1\%$, three equivalence ratios, kept constant

29 between cyclopentane and tetrahydrofuran, were studied (0.5, 1, and 2), whereas three

30 $X_{\text{fuel}}/X_{\text{O}_2}$ were investigated when $X_{\text{fuel}} = 2\%$. A detailed kinetic mechanism was developed to

31 reproduce cyclopentane and tetrahydrofuran auto-ignition. The agreement between our

32 experimental results and the modeling is very good. This mechanism was used to explain the

33 similarities and differences observed between cyclopentane and tetrahydrofuran auto-ignition.

34

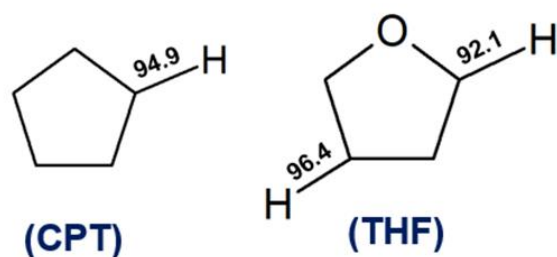
35

36 **Keywords:** Ignition delay time; shock tube; cyclopentane; tetrahydrofuran; kinetic

37 mechanism

38 1. Introduction

39 Cyclopentane (CPT) is one of the simplest cycloalkanes with five membered carbon ring,
40 which has high-octane and knock-resistant characteristics, and it is commonly found in
41 commercial gasoline [1]. Nowadays, the shift from fossil fuels to bio-fuels is an interesting
42 project for decreasing the dependence of petroleum-based fuels, and limiting the total CO₂
43 emission. Tetrahydrofuran (THF) is a saturated cyclic ether compound, and has been shown to
44 be as a promising bio-fuel for internal combustion engines [2–4]. THF has a lower heating
45 value (30.96 MJ L⁻¹) [3,4] which is close to that of CPT (33.50 MJ L⁻¹) [5], both are in the
46 vicinity of that of gasoline (~31.60 MJ L⁻¹) [2]. As seen in Figure 1, molecular structures of
47 CPT and THF are similar excluding the oxygen heteroatom in THF ring. Therefore, it is
48 critical to compare the ignition kinetics of these two molecules.



49 Figure 1: Structures of CPT and THF with bond dissociation energies (in kcal mol⁻¹)
50 calculated using ALFABET webtool [6].

51 The main numerical and experimental studies on CPT and THF auto-ignition in shock tubes
52 are summarized in Table 1.

53 Table 1: Main studies of the combustion of CPT and THF in shock tubes

Reference	Fuel	Composition	Conditions
Orme <i>et al.</i> [7]	CPT	1% CPT/O ₂ /Ar $\phi = 0.577 - 2.0$	P ₅ = 1 atm T ₅ = 1370 – 1820 K

Sajid et al. [8]	CPT	1% CPT/O ₂ /Ar $\phi = 2.0$ 1.38 – 5.30 % CPT/Air $\phi = 0.5 – 2.0$	P ₅ = 10, 20 and 40 atm T ₅ = 900 – 1650 K
Al Rashidi et al.[9]	CPT	1.4 – 5.4 % CPT/Air $\phi = 0.5 – 2.0$	P ₅ = 20 and 40 bar T ₅ = 920 – 1320 K
Dagaut et al. [10]	THF	0.5, 1% THF/O ₂ /Ar $\phi = 0.5 – 2.0$	P ₅ = 2.5, 3.5 and 5 bar T ₅ = 1000 – 1800 K
Uygun et al. [11]	THF	THF/Air $\phi = 1.0$	P ₅ = 20 and 40 bar T ₅ = 691 – 1100 K
Fenard et al. [12]	THF	THF/O ₂ /Inert mixture (N ₂ , Ar) $\phi = 1.0$	P ₅ = 0.64, 0.77, 0.91 MPa T ₅ = 691 – 1100 K
Tran et al. [2]	THF	0.25, 0.5, 1% THF/O ₂ /Ar $\phi = 0.5 – 2.0$	P ₅ = 811 – 932 kPa T ₅ = 691 – 1100 K

54

55 Many studies focusing on the comparison of the autoignition of cyclopentane with other
56 hydrocarbons have been reported in the literature [13–16]. Sirjean et al. [13] measured the
57 ignition delay times of CPT/oxygen/argon and cyclohexane/oxygen/argon mixtures in a shock
58 tube, these mixtures contained 0.5 or 1% of fuel with equivalence ratios ranging from 0.5 to
59 2.0. Temperatures and pressures behind the reflected shock waves were between 7.3–9.5 atm
60 and 1230–1840 K, respectively. These experimental data showed that the reactivity of CPT
61 was much lower than that of cyclohexane. Authors explained this observation by the
62 difference of stability of the corresponding cycloalkyl radicals. Ignition delay times of
63 CPT/air and cyclohexane/air mixtures were measured by Daley et al.[14] in a shock tube at
64 pressure of 11–61 atm, between 847–1379 K, and with equivalence ratios of 0.25, 0.5, 1.0.
65 The comparison of the reactivity between CPT and cyclohexane in this study was similar to

66 that observed in the study of Sirjean et al.[13]. Tian et al.[15] measured ignition delay times
67 of 1% cyclopentane/O₂/ and 0.833% methylcyclopentane/O₂ mixtures diluted in argon behind
68 reflected shock waves at 1.1 and 10 atm, between 1150 to 1850 K and with equivalence ratios
69 of 0.577, 1 and 2.0. Their experimental results showed that ignition delay time of
70 cyclopentane is longer than that of methylcyclopentane, especially for the fuel-lean mixture.
71 This observation was explained by the presence of the methyl group, which weakened the C-
72 C bonds of the cycle, and favored the unimolecular decomposition of methylcyclopentane.
73 Lokhachari et al. [16] investigated the impact of dimethyl ether on the ignition delay time of
74 CPT in a shock tube and a rapid compression machine. A temperature range of 650–1350 K at
75 elevated pressures of 20 and 40 bar for two mixtures (30/70 and 70/30%mol
76 cyclopentane/dimethyl ether mixture) in air were studied at equivalence ratios of 0.5, 1.0 and
77 2.0. The blending of dimethyl ether to CPT increased the reactivity of the mixture at relatively
78 lower temperatures (650–1000 K), while the reactivity was very similar at high temperatures
79 (1000–1350 K). A detailed kinetic mechanism was developed to validate the experimental
80 results.

81 Based on this literature review, the comparison of the auto-ignition of cyclopentane and
82 tetrahydrofuran has never been investigated before. Therefore, this study aims at comparing
83 the ignition delay times of CPT/O₂/Ar and THF/O₂/Ar mixtures at a pressure of 20 atm,
84 equivalence ratios ranging from lean to rich conditions (0.5, 1.0, 2.0) and with $X_{\text{fuel}}/X_{\text{O}_2}$ ratios
85 of 0.08, 0.16, 0.32. A detailed kinetic mechanism describing the oxidation of CPT and THF is
86 used in order to explain the observed differences and similarities in terms of the ignition
87 behaviors between CPT and THF.

88 **2. Experiment methods**

89 **2.1. Mixture preparation**

90 The 12 tested mixtures of CPT/O₂/Ar and THF/O₂/Ar reported in Table 2 were prepared
 91 into two stainless-steel tanks (T1 and T2 in Figure 2) based on the partial pressure method,
 92 and left to homogenize for at least 3 hours. The liquid fuels CPT with a purity of 98% and
 93 THF with a purity of 99.9% were provided by Sigma-Aldrich. High purity gases dioxygen
 94 and argon were delivered by Air-Liquide.

95 Two stainless-steel tanks are connected to the tube and vacuum system (a roughing pump and
 96 a turbo-molecular pump) through a manifold. To avoid any contamination, the vacuum
 97 system pumps down the tanks below 3 Pa prior to mixture preparation. The partial pressure of
 98 fuel in the stainless-steel tanks was 50 mbar for the case of 1% of fuel in the mixture and 100
 99 mbar for 2% of fuel. Thus, in order to avoid any condensation of the fuels, the tanks and the
 100 manifold were heated up to 40-50 °C to allow the partial pressures of CPT and THF to be at
 101 least four times lower than their vapor pressures [17]. For sake of comparison, the choice was
 102 made to maintain the equivalence ratio constant between CPT and THF experiments when 1%
 103 of fuel was used, and the $X_{\text{fuel}}/X_{\text{O}_2}$ ratio constant when 2% of fuel was used. The estimated
 104 uncertainties for the mole fractions of fuel, O₂, and Ar are 0.81%, 0.56%, and 0.2%
 105 respectively.

106

107 Table 2: Summary of the mixture composition used in this study. ϕ is the equivalence
 108 ratio, $X_{\text{fuel}}/X_{\text{O}_2}$ is the ratio of fuel and oxygen mole fractions in the mixture.

Mixture	Mixture composition (mole fraction)				ϕ	$X_{\text{fuel}}/X_{\text{O}_2}$
	CPT	THF	O ₂	Ar		
mix.1	0.010	0.000	0.150	0.840	0.50	0.067
mix.2	0.010	0.000	0.075	0.915	1.00	0.033
mix.3	0.010	0.000	0.038	0.952	2.00	0.017
mix.4	0.000	0.010	0.110	0.880	0.50	0.091
mix.5	0.000	0.010	0.055	0.935	1.00	0.046
mix.6	0.000	0.010	0.027	0.963	2.00	0.023

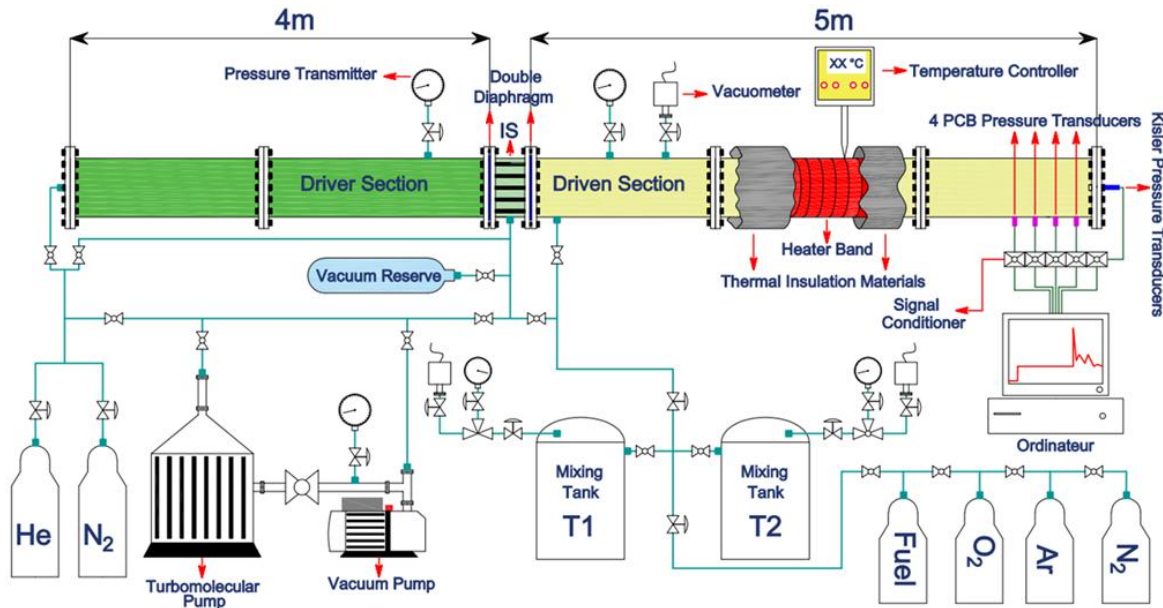
mix.7	0.020	0.000	0.250	0.730	0.60	0.080
mix.8	0.020	0.000	0.125	0.855	1.20	0.160
mix.9	0.020	0.000	0.063	0.917	2.40	0.320
mix.10	0.000	0.020	0.250	0.730	0.44	0.080
mix.11	0.000	0.020	0.125	0.855	0.88	0.160
mix.12	0.000	0.020	0.063	0.917	1.76	0.320

109

110 2.2. Ignition delay time measurements

111 The ignition delay times of the CPT/O₂/Ar and THF/O₂/Ar mixtures are measured in a
112 high-pressure shock tube in DRIVE [18] over a temperature range of 865–1700 K at 20 atm.
113 As presented in Figure 2, the tube consists of a stainless-steel tube (inner diameter of 50 mm)
114 and separated into two parts (driver section 4 m and driven section 5 m) by a double stainless-
115 steel diaphragm. The position of the shock wave is measured using four piezoelectric pressure
116 transducers (PCB 113B22) located in the last part of the driven section. The post-shock
117 pressure is recorded by using an additional piezoelectric pressure transducer (Kistler 603B1)
118 positioned at the end-wall.

119 Helium was used as the driver gas. The driven section was heated up to 40–50 °C to avoid
120 any condensation of CPT or THF during the measurements. The diaphragm thickness ranging
121 from 200 to 300 μm are used. The rupture of both diaphragms, creating the shock wave, was
122 performed using the vacuum reserve leading to an immediate pressure decrease in the
123 intermediate section. To prevent any contamination of the tested mixture during the
124 experiment, the tube is pumped down below 5 Pa.

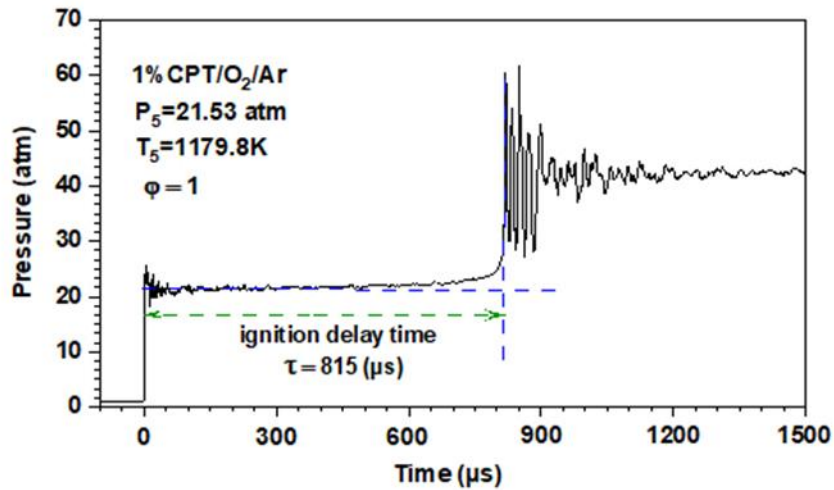


125 Figure 2: Schematic diagram of the high-pressure shock tube apparatus in DRIVE laboratory.

126

127 The method used to identify the ignition delay time in this study is explained in more detail in
 128 [18]. Pressure profiles recorded by the pressure transducers (PCB 113B22) are used to
 129 determine the ignition delay time as presented in Figure 3. The ignition delay time is inferred
 130 by the crossing between the horizontal line at p_5 and the tangent line to the pressure trace at
 131 the maximum pressure increase. The post-shock pressure, p_5 and post-shock temperature T_5 ,
 132 were calculated from the shock wave velocity and the initial conditions based on the 1-D
 133 shock relations and the species thermodynamics using the chemical equilibrium software
 134 Gaseq [22]. The difference between the post-shock pressure p_5 calculated by Gaseq and that
 135 of the experimental pressure trace is below $\pm 4\%$. The accuracy of the post-shock temperature
 136 T_5 is $\pm 1\%$ which corresponds to $\pm 8-15$ K. The estimated uncertainty for the measured
 137 pressure p_5 is approximately 1.5%.

138



139 Figure 3: Definition of ignition delay time

140 In the shock tube experiment, several non-ideal effects influence the measurement of ignition
 141 delay time. The displacement of the reflected shock wave creates a boundary layer behind it,
 142 affecting the pressure and temperature p_5 and T_5 . The overall uncertainty in ignition delay
 143 time was influenced by multiple factors, including uncertainties in reflected shock conditions,
 144 variations in mixture preparation, and the precision of ignition delay determination from
 145 measured signals. This uncertainty is approximately $\pm 20\%$.

146

147 3. Kinetic modeling and simulation method

148 Shock tube simulations were performed using ANSYS Chemkin 2022 R2 [23] with the
 149 constant volume assumption. Computed ignition delay times were determined from calculated
 150 pressure profiles by the method presented in section 2.2. For the longest ignition delay times,
 151 a pressure rise was observed between the reflected shock and the auto-ignition. The impact of
 152 the pressure rise on ignition delay times has been discussed elsewhere [24, 25]. A negative
 153 heat loss (i.e. a heat gain) of $-20 \text{ cal s}^{-1} < \dot{Q} < -50 \text{ cal s}^{-1}$ was introduced as an input in
 154 Chemkin in order to account for the pressure rise experimentally observed ($2.4\% / \text{ms} < dp/dt$
 155 $< 7.5\% / \text{ms}$). For a given mixture, the same heat gain is used. For each of the 12 tested
 156 mixtures the value of the heat gain was adapted in order to reproduce the experimental

157 pressure rise. The longest ignition delay times of CPT and THF were clearly influenced by the
158 heat gain while this impact was not observed for shorter ignition delay times (see Figures S1
159 and S2 in the Supplementary Material).

160 The kinetic mechanism used in the simulations was developed by merging a mechanism for
161 THF from Fenard *et al.* [12] and a mechanism for CPT from Lokhachari *et al.* [16]. The
162 kinetic and thermodynamic data of the common reactions and species in both mechanisms
163 were taken from Fenard *et al.* [12]. The list of common species and reactions is presented in
164 the Supplementary Material. Indeed, doing so has no impact on the performance of
165 Lokhachari *et al.* sub-mechanism to model CPT auto-ignition and preserve the capability of
166 Fenard *et al.* sub-mechanism to reproduce THF ignition delays (see Figures S3 and S4 in the
167 Supplementary Material). On the contrary, keeping the kinetic and thermodynamic data from
168 Lokhachari *et al.* for common reactions and species yield an overprediction of the ignition
169 delay times of THF. The origin of this discrepancy would be interesting to investigate but is
170 beyond the scope of this study.

171 The present mechanism contains 1322 species and 6709 reactions and is available with its
172 thermodynamic data in Chemkin format in supplementary material.

173

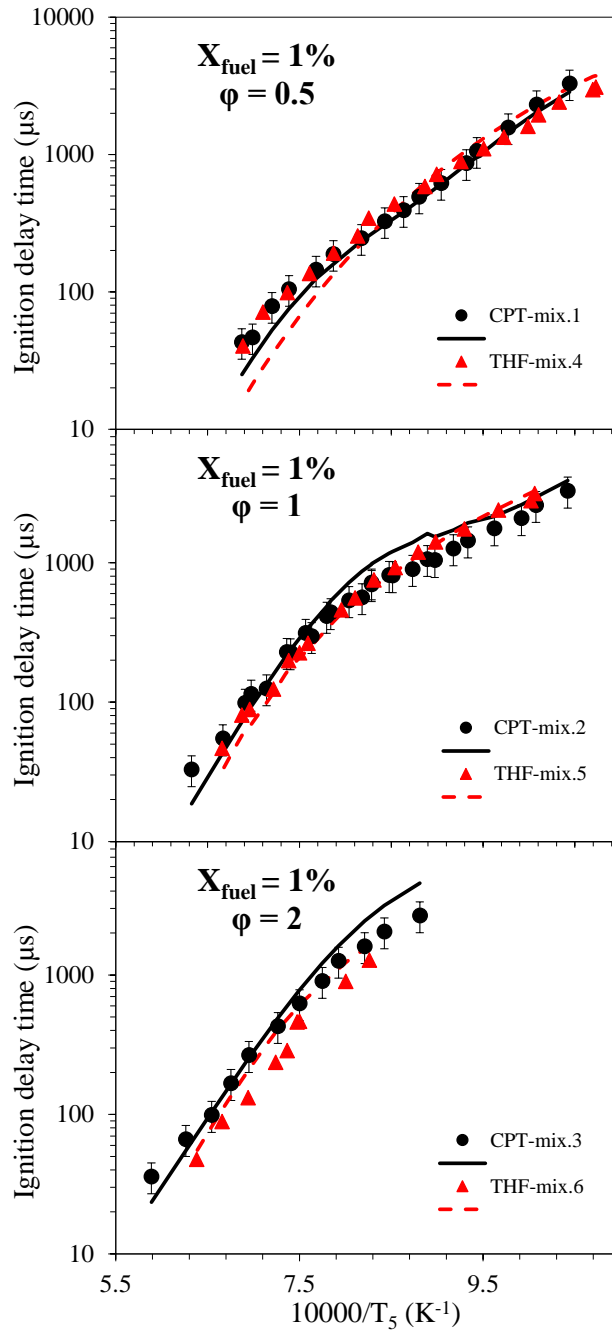
174 **4. Results and discussion**

175 A vertical error bar of 25% was applied to present experimental data, accounting for
176 uncertainties of our experimental set-up and mixture preparation. The shortest and the longest
177 ignition delay times are the measurement limits with these two molecules for each condition
178 in our experimental device.

179 **4.1 $X_{Fuel} = 1\%$**

180 Figure 4 presents the comparison of reactivity between CPT and THF for different
181 mixtures in shock tube at 20 atm. As can be seen in this figure, cyclopentane (CPT) and

182 tetrahydrofuran (THF) have very similar ignition delay times with 1% of fuel, THF being
183 slightly more reactive at $\phi = 2$. It can also be seen that the proposed kinetic mechanism is very
184 well able to capture the observed trends, the ignition delay times of THF being
185 underestimated under fuel-lean conditions at high-temperature. This mechanism was thus
186 used to identify the reaction pathways involved in the auto-ignition of CPT and THF in order
187 to highlight the reason why they behave similarly despite weaker C-H bond dissociation
188 energies on the α -carbons of THF.



189

190 Figure 4: CPT (black) and THF (red) ignition delay times vs. $10000/T_5$ for $X_{fuel} = 1\%$, $p_5 = 20$

191 atm, and three different equivalence ratios.

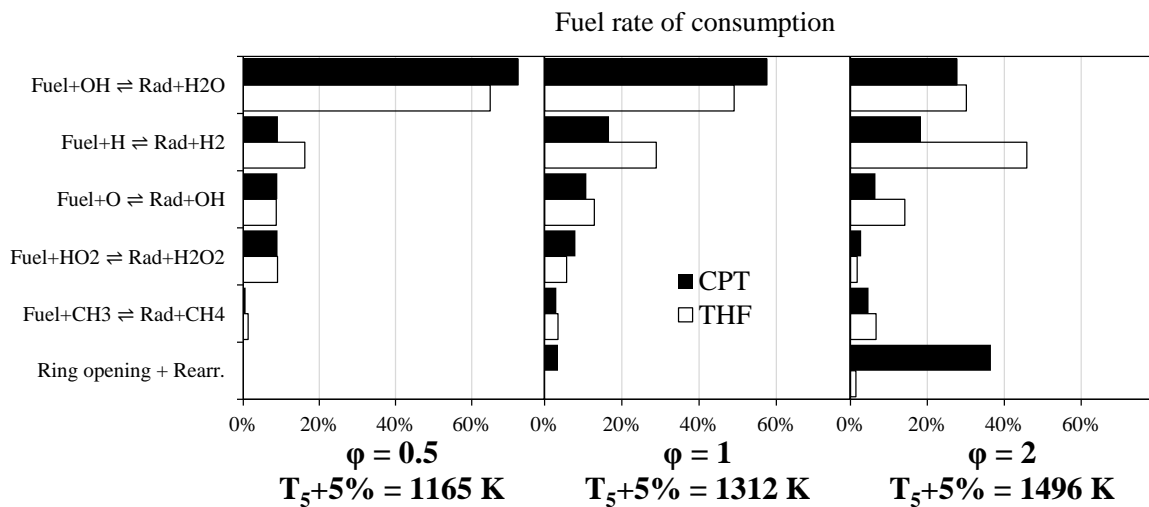
192 Although CPT and THF have very similar ignition delay times with 1% of fuel, it turns out

193 that the chain of reactions eventually leading to the ignition of the mixtures is significantly

194 different. Reaction pathway analyses were performed at $\phi = 0.5$, $T_5 = 1110$ K, at $\phi = 1$, $T_5 =$

195 1250 K, and at $\phi = 2$, $T_5 = 1425$ K, for both CPT and THF, when the temperature increase

196 reaches 5% of the initial T_5 . The choice of this criterion was made in order to compare
 197 cyclopentane and tetrahydrofuran reactivity for a given mixture composition at the same
 198 temperature, since temperature is a key parameter in kinetics. On the other hand, because of
 199 this choice, it is not possible to compare these analyses for a same fuel at different
 200 equivalence ratios. Here, the focus is on the differences and similarities between CPT and
 201 THF reactivity for each condition.

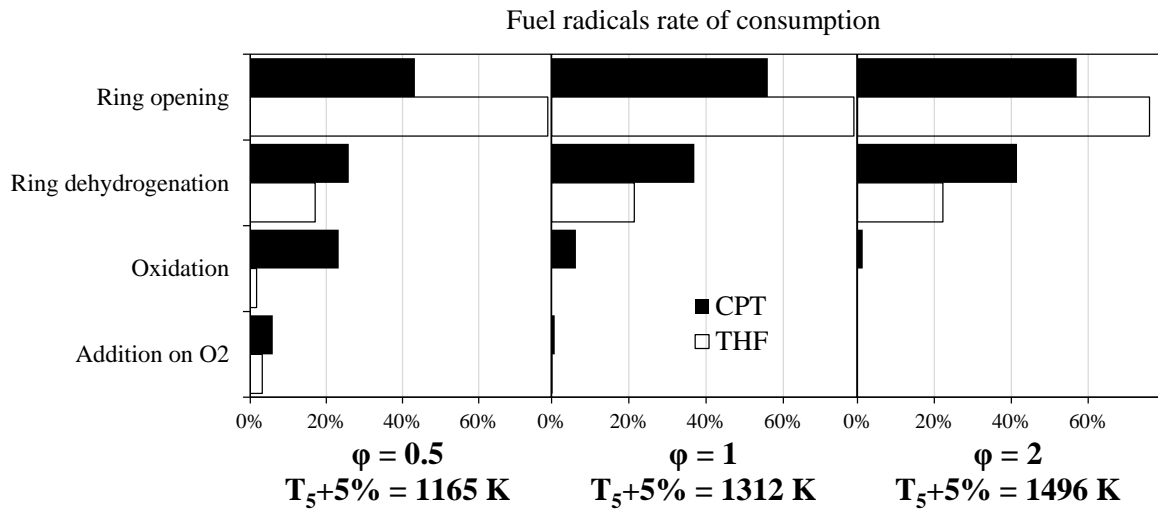


202
 203 Figure 5: Main pathways of CPT and THF consumption at $\phi = 0.5, 1, \text{ and } 2$ for $X_{fuel} = 1\%$,
 204 and $P_5 = 20$ atm. *Rad* is cyclopentyl for CPT and the sum of α - and β -tetrahydrofuranyl for THF - *Rearr.*
 205 stands for rearrangement.

206 Figure 5 shows that, under fuel-lean and stoichiometric conditions, both CPT and THF are
 207 mostly consumed by H-abstraction reactions by OH, CPT being slightly more consumed by
 208 OH than THF. On the contrary, THF is more consumed than CPT by H-abstraction reactions
 209 by H atoms. It means that, under these conditions, both fuels are able to generate enough
 210 radicals to be consumed approximately at the same pace. Under fuel-rich conditions, among
 211 H-abstraction reactions, OH still dominates CPT consumption, but cyclopentane is more
 212 consumed by the ring opening reaction followed by a rearrangement yielding 1-pentene.
 213 Under the same conditions, THF is mostly consumed by H-abstraction reactions by H,

214 followed by OH. Unlike CPT, ring opening, has virtually no role as an initiation step in the
 215 case of THF. It shows that the radical pool has less influence on the ignition process in the
 216 case of CPT than for THF under fuel-rich conditions.

217 The fate of the fuel radicals is presented by Figure 6. It turns out that, regardless of the
 218 conditions, ring opening is always the dominant pathway for THF, the formation of
 219 dihydrofurans (mostly by C-H β -scission) being rather limited. As far as cyclopentyl radical is
 220 concerned, ring opening reaction is also dominant for fuel-rich and stoichiometric mixtures,
 221 however since ring dehydrogenation and oxidation preserve the ring structure, ring opening is
 222 not dominant under fuel-lean conditions. Therefore, the radical pool necessary to consume
 223 THF is obtained from ring opening and subsequent reactions whereas, for CPT, the ring
 224 structure indeed participates to the formation of the small radicals.

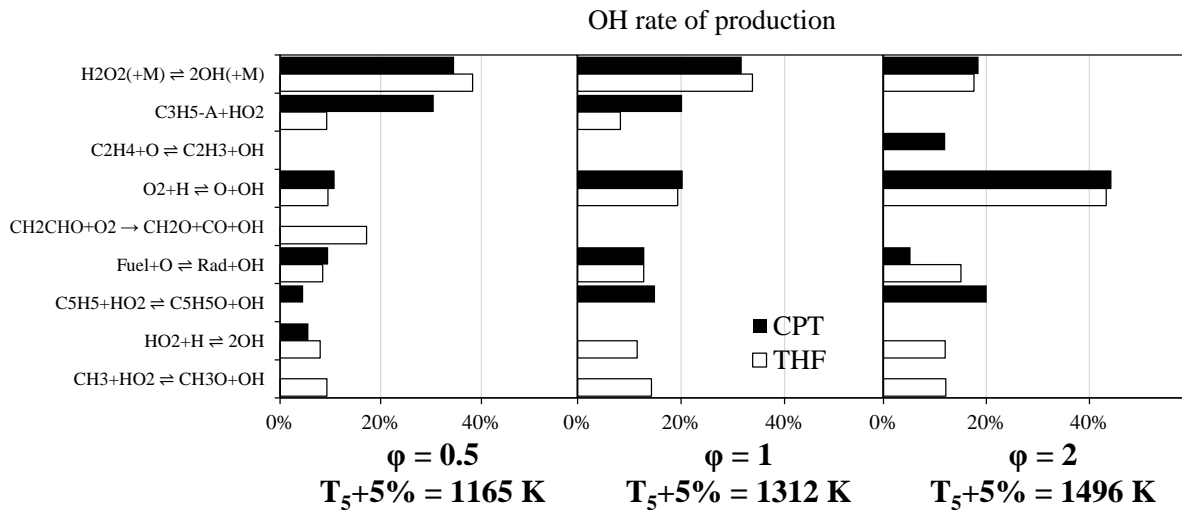


225
 226 Figure 6: Main consumption pathways for cyclopentyl, and α - and β -tetrahydrofuranyl
 227 radicals at $\phi = 0.5, 1, \text{ and } 2$ for $X_{fuel} = 1\%$, and $p_5 = 20$ atm.

228 **- Role of OH:**

229 As commonly observed, under fuel-lean conditions, OH is a key radical to consume
 230 both CPT and THF. Figure 7 shows that, for both fuels, the decomposition of H_2O_2 is a major

231 OH provider However, while in the case of CPT the second most important OH providers are
232 the reactions $C_3H_5-a + HO_2 \rightleftharpoons C_3H_5O + OH$ and $C_3H_5OOH \rightleftharpoons C_3H_5O + OH$, almost 20% of
233 OH comes from $CH_2CHO + O_2 \rightarrow CH_2O + CO + OH$. In the case of THF, vinoxy radicals are
234 essentially formed from α -tetrahydrofuranyl after ring opening. The reaction $CH_2CHO + O_2$
235 $\rightarrow CH_2O + CO + OH$ makes THF less dependent on HO_2 to produce OH than CPT. The share
236 of $H + O_2 \rightleftharpoons OH + O$ and $Fuel + O \rightleftharpoons Rad + OH$, (Rad: cyclopentyl for CPT, and the sum of
237 α - and β -tetrahydrofuranyl for THF), in OH production is almost the same for both fuels.
238 Finally, the role of allyl radical in OH production is less important for THF than for CPT
239 because when cyclopentyl opens, it only yields allyl after β -scission, while β -
240 tetrahydrofuranyl is the only radical able to produce allyl, the α -tetrahydrofuranyl, the most
241 abundant one, producing mainly vinoxy radicals. In addition, it can be noticed that the sum of
242 the contributions of vinoxy and allyl radicals produces relatively less OH for THF than allyl
243 alone for CPT. Although the temperatures of the analyses are different, more or less the same
244 picture can be drawn for the stoichiometric mixture except that the role of vinoxy + O_2
245 decreases for THF and $H + O_2$ increases for both fuels. Under fuel-rich conditions, OH is
246 mostly produced from $H + O_2 \rightleftharpoons OH + O$ for both fuels with the same share. The role of H_2O_2
247 dissociation is also very similar between CPT and THF. The difference lies on $C_5H_5 + HO_2$
248 and the H-abstraction from C_2H_4 by O atoms, which are respectively the third and fourth most
249 important OH production routes for CPT, whereas OH is produced by THF + O H-abstraction
250 reactions, $HO_2 + H \rightleftharpoons 2 OH$, and $CH_3 + HO_2 \rightleftharpoons CH_3O + OH$ in addition to $H + O_2 \rightleftharpoons OH +$
251 O and H_2O_2 dissociation for THF.



252

253 Figure 7: Main pathways of OH production for CPT and THF at $\phi = 0.5, 1, \text{ and } 2$ for $X_{fuel} =$
 254 1% , and $p_5 = 20 \text{ atm}$. Rad is cyclopentyl for CPT and the sum of α - and β -tetrahydrofuranlyl for THF, and
 255 $C_3H_5-A + HO_2$ stands for the sum of $C_3H_5-a + HO_2 \rightleftharpoons C_3H_5O + OH$ and $C_3H_5OOH \rightleftharpoons C_3H_5O + OH$.

256 To summarize the role of OH, H₂O₂ dissociation and $H + O_2 \rightleftharpoons OH + O$ have similar shares
 257 for CPT and THF regardless of the equivalence ratio, and this flux represents between 45 %
 258 and 62 % of the total OH rate of production. This appears to be sufficient for cyclopentane
 259 and tetrahydrofuran to ignite after a similar delay in addition to:

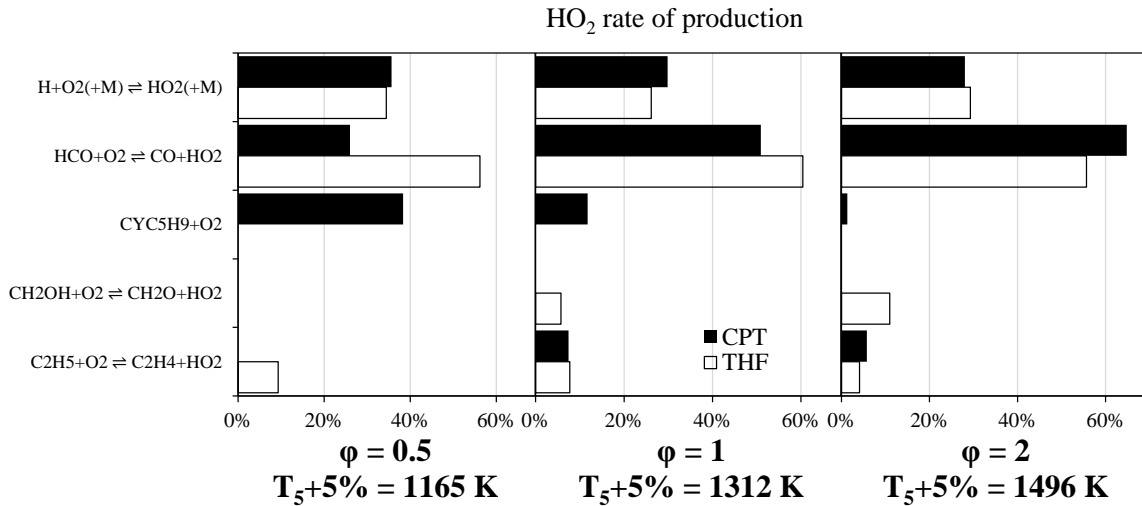
260 - under fuel-lean conditions, the production of OH from $C_3H_5-a + HO_2$ in CPT oxidation is
 261 compensated by $CH_2CHO + O_2 \rightarrow CH_2O + CO + OH$ and $CH_3 + HO_2 \rightleftharpoons CH_3O + OH$ in THF
 262 oxidation.

263 - for a stoichiometric mixture, the additional OH comes from $C_3H_5-a + HO_2$ and $C_5H_5 + HO_2$
 264 for CPT, whereas $H + HO_2 \rightleftharpoons 2 OH$ and $CH_3 + HO_2 \rightleftharpoons CH_3O + OH$ produce the additional
 265 OH for THF, showing again the strong influence of HO₂ on the ignition of both fuels, and the
 266 role of allylic radicals for CPT and small radicals for THF.

267 - under fuel-rich conditions, $\text{H} + \text{HO}_2$, $\text{CH}_3 + \text{HO}_2$, and $\text{THF} + \text{O}$ are responsible for the extra
268 OH production for THF while, in the case of CPT, it relies on $\text{C}_5\text{H}_5 + \text{HO}_2$ and $\text{C}_2\text{H}_4 + \text{O} \rightleftharpoons$
269 $\text{C}_2\text{H}_3 + \text{OH}$.

270 **- Role of HO_2 :**

271 H_2O_2 , which plays a significant role in the production of OH for CPT as well as for
272 THF for the fuel-lean and stoichiometric mixtures, mostly comes from the H-abstraction
273 reaction on the fuel by HO_2 and the dismutation of HO_2 with itself. It is therefore ultimately
274 HO_2 which has a preponderant role in the production of OH under these conditions. As can be
275 seen in Figure 8, $\text{H} + \text{O}_2 (+\text{M}) \rightleftharpoons \text{HO}_2 (+\text{M})$ has a very similar share in terms of HO_2
276 production between CPT and THF regardless of the equivalence ratio (and the temperature).
277 However, under fuel-lean conditions, 38% of HO_2 comes from the oxidation of cyclopentyl
278 radicals (including direct oxidation by O_2 and concerted elimination of HO_2 after O_2
279 addition), and 26% from $\text{HCO} + \text{O}_2$, whereas for THF, $\text{HCO} + \text{O}_2$ dominates the production
280 of HO_2 (56%), $\text{C}_2\text{H}_5 + \text{O}_2$ playing a minor role (9%). For the stoichiometric mixture, more
281 HO_2 is produced from $\text{HCO} + \text{O}_2$ in the case of THF, but CPT compensate with the oxidation
282 of cyclopentyl radicals. Finally, under fuel-rich conditions, almost two third of the HO_2 comes
283 from $\text{HCO} + \text{O}_2$ for CPT, which is more than THF, but THF compensate producing also HO_2
284 from $\text{CH}_2\text{OH} + \text{O}_2 \rightleftharpoons \text{CH}_2\text{O} + \text{HO}_2$.



285

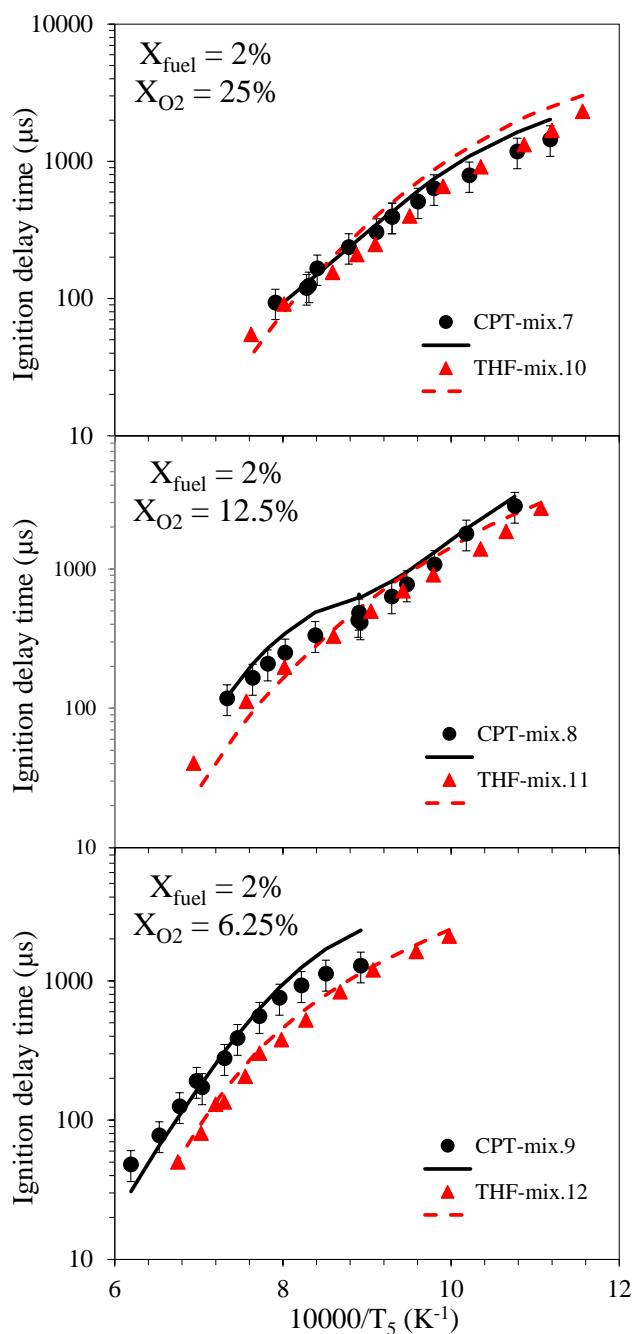
286 Figure 8: Main pathways of HO₂ production for CPT and THF at $\phi = 0.5, 1, \text{ and } 2$ for $X_{fuel} =$
 287 1% , and $p_5 = 20 \text{ atm}$. *CYC5H9 + O₂* stands for the sum of the direct oxidation by O₂ and the concerted
 288 elimination of HO₂ after O₂ addition.

289 To summarize on the role of HO₂, ring opening is a very important pathway in the
 290 consumption of THF. It is made easier as compared to CPT by the presence of the O atom. It
 291 finally yields high amounts of formyl radicals which in turn produce HO₂, strongly related to
 292 OH formation, and thus THF consumption (and ignition) under the explored conditions. For
 293 CPT, the picture is more complicated. Under fuel-lean conditions and lower temperature, the
 294 ring is preserved and HO₂ is formed by oxidation of cyclopentyl radicals. This, however,
 295 takes a similar time to occur as in the case of THF. For stoichiometric and fuel-rich mixtures,
 296 where ring opening dominates cyclopentyl consumption, HO₂ is formed, as for THF, mostly
 297 from HCO which comes from the regular pathway for alkanes through CH₂O, C₂H₃, and C₂H₄
 298 making CPT to auto-ignite like THF does.

299 **4.2 X_{Fuel} = 2 %**

300 Figure 9 presents a comparison of the ignition delay times of CPT and THF for
 301 different mixtures in shock tube at 20 atm. As can be seen from this figure, cyclopentane
 302 (CPT) and tetrahydrofuran (THF) have again very similar ignition delay times with 25% of

303 O₂, and 12.5% of O₂ at low temperature. However, cyclopentane ignites later than
304 tetrahydrofuran with 12.5% of O₂ at high temperature and with 6.25% of O₂. It can also be
305 seen in Fig. 9 that the kinetic mechanism is still well able to capture the observed trends, and
306 particularly the ignition delay of CPT. Therefore, this mechanism was used to identify the
307 reaction pathways involved in the auto-ignition of CPT and THF in order to highlight the
308 reason of the delay observed for CPT. Four reaction pathway analyses were performed at X_{O₂}
309 = 25%, T₅ = 1000 K, at X_{O₂} = 12.5%, T₅ = 1000 K and 1335 K, and at X_{O₂} = 6.25%, T₅ =
310 1335 K, both for CPT and THF, with the same criterion on the temperature increase of 5% as
311 when X_{fuel} = 1%. With this choice of T₅, comparisons can also be done between X_{O₂} = 25%
312 and X_{O₂} = 12.5% at 1000 K, and also between X_{O₂} = 12.5% and X_{O₂} = 6.25% at 1335 K.

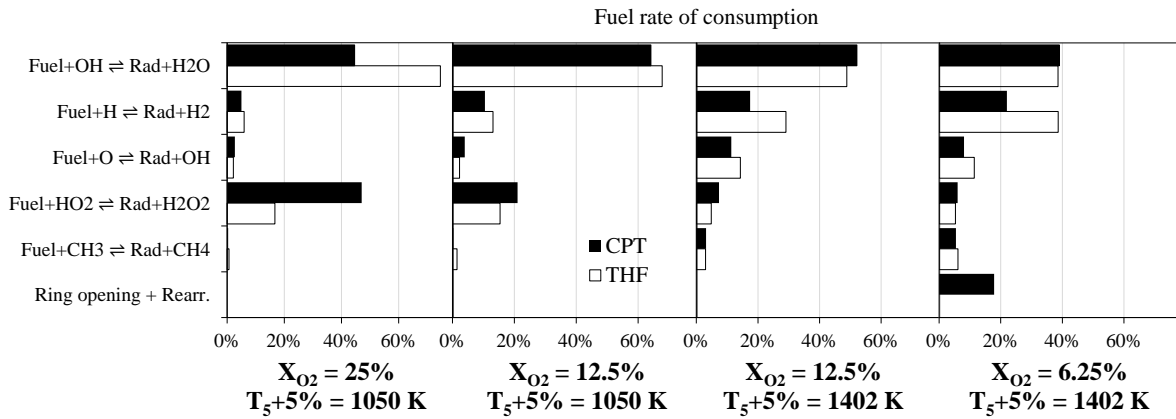


313

314 Figure 9: CPT (black) and THF (red) ignition delay times vs. $10000/T_5$ for $X_{fuel} = 2\%$, $p_5 = 20$
 315 atm, and three different O_2 initial mole fractions.

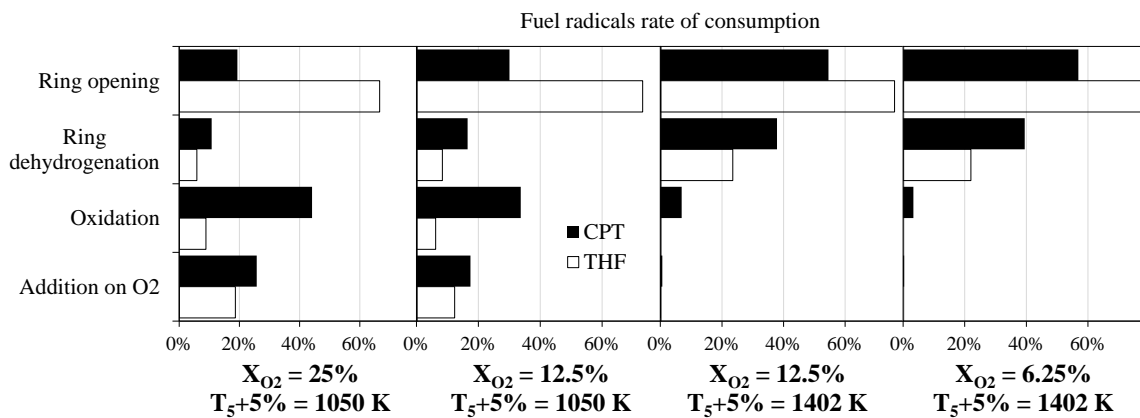
316 Figure 10 shows that, when $X_{O_2} = 25\%$, THF is mostly consumed by OH while CPT is half
 317 consumed by OH and half by HO_2 . The share of HO_2 in the consumption of CPT decreases
 318 with the mole fraction of O_2 while that of H increases. It can also be noticed that the reaction
 319 producing 1-pentene from cyclopentane (ring opening + rearrangement) consumes 18% of

320 CPT when $X_{O_2} = 6.25\%$ while such a reaction does not occur for THF. OH is again of major
 321 importance in the consumption of both CPT and THF, HO_2 playing a non-negligible role for
 322 CPT with high O_2 content as well as H atoms for THF with low O_2 content.



323
 324 Figure 10: Main pathways of CPT and THF consumption at $X_{O_2} = 25\%$, 12.5% , and 6.25%
 325 for $X_{fuel} = 2\%$, and $p_5 = 20\text{ atm}$. Rad is cyclopentyl for CPT and the sum of α - and β -tetrahydrofuranlyl for
 326 THF - Rearr. stands for rearrangement.

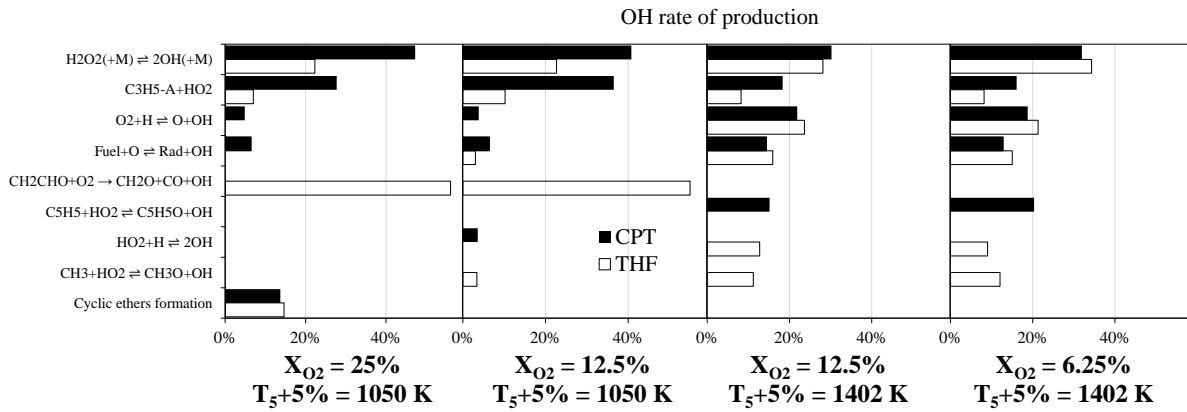
327 Under these conditions, the relative rates of consumption of the fuel radicals are presented in
 328 Figure 11. It turns out that the fate of cyclopentyl and tetrahydrofuranlyls is very similar to
 329 what was observed when $X_{fuel} = 1\%$, tetrahydrofuranlyls being mostly consumed by ring
 330 opening whereas the C5 ring is maintained at lower temperature and opens at higher
 331 temperature, when CPT is delayed as compared to THF.



332

333 Figure 11: Main consumption pathways for cyclopentyl, and α - and β -tetrahydrofuranyl at
 334 $X_{O_2} = 25\%$, 12.5% , and 6.25% for $X_{fuel} = 2\%$, and $p_5 = 20$ atm.

335 **- Role of OH:**



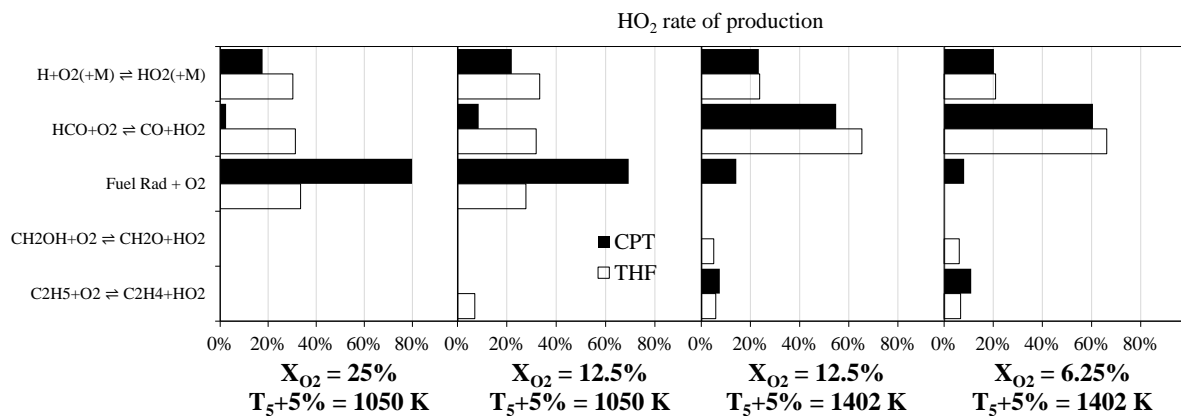
336
 337 Figure 12: Main pathways of OH production for CPT and THF at $X_{O_2} = 25\%$, 12.5% , and
 338 6.25% for $X_{fuel} = 2\%$, and $p_5 = 20$ atm. *Rad* is cyclopentyl for CPT and the sum of α - and β -
 339 tetrahydrofuranyl for THF, and $C_3H_5-A + HO_2$ stands for the sum of $C_3H_5-a + HO_2 \rightleftharpoons C_3H_5O + OH$ and
 340 $C_3H_5OOH \rightleftharpoons C_3H_5O + OH$.

341 Surprisingly enough, the reaction pathways producing OH are significantly different
 342 between CPT and THF when they have similar ignition delay times ($X_{O_2} = 25\%$, and $X_{O_2} =$
 343 12.5% at $T_5 = 1000$ K) whereas they are less different when CPT ignition is delayed as
 344 compared to THF ($X_{O_2} = 12.5\%$ at $T_5 = 1335$ K, and $X_{O_2} = 6.25\%$), as can be seen from
 345 Figure 12. For CPT, the dominant pathways for OH production lie on HO_2 , either directly by
 346 reaction with allyl radicals or through H_2O_2 formation. For THF, H_2O_2 dissociation accounts
 347 only for a quarter of OH production, more than half of it coming from the reaction of vinyloxy
 348 radicals and O_2 ($CH_2CHO + O_2 \rightarrow CH_2O + CO + OH$). Thus, when CPT and THF ignite after
 349 equivalent times, OH production pathways are significantly different, CPT relying more on
 350 HO_2 and THF directly on the O_2 content. However, when CPT is delayed, it comes out that

351 resonantly stabilized allylic radicals (allyl and cyclopentadienyl radicals) are involved in OH
 352 production for CPT while H and CH₃ are involved in the case of THF.

353 **- Role of HO₂:**

354 HO₂ is thus a key intermediate in the production of OH under all tested conditions for
 355 CPT, and at high-temperature and low O₂ content for THF. With a doubled initial amount of
 356 fuel, the oxidation of cyclopentyl, either directly or through addition on O₂ and concerted
 357 elimination of HO₂, gained in importance to produce HO₂ for CPT at low temperature and
 358 high O₂ content. Under the same conditions, a third of the HO₂ production for THF relies on
 359 H + O₂ (+M), another third on HCO + O₂, and the last third comes from tetrahydrofuranyl
 360 radicals oxidation. At higher temperature and lower O₂ content, when CPT is delayed
 361 compared to THF, the reaction pathways yielding HO₂ are very similar between cyclopentane
 362 and tetrahydrofuran, HCO + O₂ producing slightly more HO₂ in the case of THF than for
 363 CPT.



364
 365 Figure 13: Main pathways of HO₂ production for CPT and THF at X_{O₂} = 25%, 12.5%, and
 366 6.25% for X_{fuel} = 2%, and p₅ = 20 atm. Fuel Rad + O₂ stands for the sum of the direct oxidation by O₂
 367 and the concerted elimination of HO₂ after O₂ addition.

368 It turns out that ring opening seems to be responsible for cyclopentane to be delayed as
369 compared to tetrahydrofuran. As far as THF is concerned, the ring opening from the α -
370 tetrahydrofuranyl radical, the most abundant one, produces vinoxy radicals, which in turn
371 produce OH by reaction with O₂, at low temperature and high O₂ content, or produce H atoms
372 (+ ketene) and CH₃ (+ CO) at high temperature and low O₂ content. This sequence of
373 reactions generates the OH required for the consumption of THF by different, but efficient,
374 pathways. For CPT, at low temperature and high O₂ content, the ring is preserved allowing
375 HO₂ to be produced by reaction between cyclopentyl radicals and O₂, generating OH radicals
376 to consume CPT as fast as THF is. However, ring opening produces allyl radicals which are
377 most likely to be consumed by HO₂, but the ring opens at high temperature, where HO₂ is
378 much less produced. Therefore, resonantly stabilized allyl radicals, with less partners to react
379 with, stifle the reactivity, and cyclopentane ignition is delayed as compared with
380 tetrahydrofuran.

381

382 **5. Conclusion**

383 This study reports the comparison between cyclopentane and tetrahydrofuran auto-ignition in
384 a high-pressure shock tube. New ignition delay times were measured at 20 atm and various
385 equivalence ratios and initial fuel mole fractions. A detailed kinetic mechanism was
386 developed in order to reproduce the experimental observations. Since the agreement was
387 found to be good, this mechanism was used to explain the similarities and differences between
388 cyclopentane and tetrahydrofuran in terms of auto-ignition. It turns out that cyclopentane and
389 tetrahydrofuran exhibit very similar behaviors under most of the tested conditions, only at
390 high-temperature and low O₂ content, cyclopentane ignition is delayed. Reaction pathway
391 analyses were performed and showed that, in the case of tetrahydrofuran, the ring is made
392 easier to open by the presence of the oxygen atom, and the subsequent reactions of vinoxy

393 radicals support the production of HO₂, H, and OH radicals. In the case of cyclopentane,
394 higher temperatures are required to open the ring but the production of HO₂ is supported by
395 the oxidation of cyclopentyl radicals and that of OH by the reactions between resonantly
396 stabilized allyl and cyclopentadienyl radicals with HO₂. On the contrary, when temperature
397 increases and O₂ content decreases, ring opening is favored, increasing the production of allyl
398 radicals but, HO₂, a key intermediate in allyl consumption, formation decreases, thus delaying
399 the ignition of cyclopentane.

400

401

402 **Acknowledgements**

403 Authors gratefully acknowledge funding received from The Bourgogne Franche-Comté
404 Council and Labex Caprysses (convention ANR-11-LABX-0006-01).

405

406 **References**

- 407 [1] Knocking characteristics of pure hydrocarbons, ASTM, API Research Project No. 45,
408 API, 1958.
- 409 [2] Tran LS, Verdicchio M, Monge F, Martin RC, Bounaceur R, Sirjean B, Glaude PA,
410 Alzueta MU, Battin-Leclerc F. An experimental and modeling study of the combustion of
411 tetrahydrofuran. *Combust Flame* 2015;162:1899-1918.
- 412 [3] Huang J, Xiao H, Yang X, Guo F. Combustion Characteristics and Emission Analysis of
413 Tetrahydrofuran–Biodiesel-Blended Fuel in a Diesel Engine. *Energy Fuels* 2021;35:3164-
414 3173.
- 415 [4] Aydoğan B. Experimental investigation of tetrahydrofuran combustion in homogeneous
416 charge compression ignition (HCCI) engine: Effects of excess air coefficient, engine
417 speed and inlet air temperature. *J Energy Inst* 2020;93:1163-1176.
- 418 [5] Thermal-FluidsPedia | Heat of Combustion | Thermal-Fluids Central.
419 http://www.thermalfluidscentral.org/encyclopedia/index.php/Heat_of_Combustion.
420 Accessed July 14, 2022.

- 421 [6] St. John PC, Guan Y, Kim Y, Kim S, Paton RS. Prediction of organic homolytic bond
422 dissociation enthalpies at near chemical accuracy with sub-second computational cost.
423 *Nat Commun* 2020;11:2328.
- 424 [7] Orme J, Curran HJ, Simmie JM. Shock Tube Study of 5 Membered Cyclic Hydrocarbon
425 Oxidation. *European Combustion Meeting*, Chania, Greece, 2005.
- 426 [8] Sajid MB, Al Rashidi MJ, Mehl M, Pitz WJ, Sarathy SM, Farooq A. Reaction Kinetics
427 Shock Tube Ignition Measurements and Modeling of Cyclopentane. *9th U.S. National
428 Combustion Meeting*, Cincinnati, Ohio, 2015.
- 429 [9] Al Rashidi MJ, Mármol JC, Banyon C, Sajid MB, Mehl M, Pitz WJ, Mohamed S,
430 Alfazazi A, Lu T, Curran HJ, Farooq A, Sarathy SM. Cyclopentane combustion. Part II.
431 Ignition delay measurements and mechanism validation. *Combust Flame* 2017;183:372-
432 385.
- 433 [10] Dagaut P, McGuinness M, Simmie JM, Cathonnet M. The Ignition and Oxidation of
434 Tetrahydrofuran: Experiments and Kinetic Modeling. *Combust Sci Technol* 1998;135:3-
435 29.
- 436 [11] Uygun Y, Ishihara S, Olivier H. A high-pressure ignition delay time study of 2-
437 methylfuran and tetrahydrofuran in shock tubes. *Combust Flame* 2014;161:2519-2530.
- 438 [12] Fenard Y, Gil A, Vanhove G, Carstensen HH, Van Geem KM, Westmoreland PR,
439 Herbinet O, Battin-Leclerc F. A model of tetrahydrofuran low-temperature oxidation
440 based on theoretically calculated rate constants. *Combust Flame* 2018;191:252-269.
- 441 [13] Sirjean B, Buda F, Hakka H, Glaude PA, Fournet R, Warth V, Battin-Leclerc F, Ruiz-
442 Lopez M. The autoignition of cyclopentane and cyclohexane in a shock tube. *Proc
443 Combust Inst* 2007;31:277-284.
- 444 [14] Daley SM, Berkowitz AM, Oehlschlaeger MA. A shock tube study of cyclopentane
445 and cyclohexane ignition at elevated pressures. *Int J Chem Kinet* 2008;40:624-634.
- 446 [15] Tian Z, Tang C, Zhang Y, Zhang J, Huang Z. Shock Tube and Kinetic Modeling Study
447 of Cyclopentane and Methylcyclopentane. *Energy Fuels* 2015;29:428-441.
- 448 [16] Lokachari N, Wagnon SW, Kukkadapu G, Pitz WJ, Curran HJ. An experimental and
449 kinetic modeling study of cyclopentane and dimethyl ether blends. *Combust Flame*
450 2021;225:255-271.
- 451 [17] Yaws CL, Satyro MA. Chapter 1 - Vapor Pressure – Organic Compounds, Yaws
452 Handb. Vap. Press. Second Ed. Gulf Professional Publishing; 2015. 1-314 p.
- 453 [18] El Merhubi H, Kéromnès A, Catalano G, Lefort B, Le Moyne L. A high pressure
454 experimental and numerical study of methane ignition. *Fuel* 2016;177:164-172.

- 455 [19] Campbell MF, Parise T, Tulgestke AM, Spearrin RM, Davidson DF, Hanson RK.
456 Strategies for obtaining long constant-pressure test times in shock tubes. *Shock Waves*
457 2015;25:651-665.
- 458 [20] Amadio AR, Crofton MW, Petersen EL. Test-time extension behind reflected shock
459 waves using CO₂-He and C₃H₈-He driver mixtures. *Shock Waves* 2006;16:157-165.
- 460 [21] WiSTL x-t Diagram.
461 <http://silver.neep.wisc.edu/~shock/tools/xt.html>. Accessed November 4, 2021.
- 462 [22] Gaseq Chemical Equilibrium Program.
463 <http://www.gaseq.co.uk/>. Accessed October 17, 2021.
- 464 [23] Ansys Chemkin-Pro 2022 R2 | Chemical Kinetics Simulation Software.
- 465 [24] Nativel D, Cooper SP, Lipkowitz T, Fikri M., Petersen EL, Schulz C. Impact of
466 shock-tube facility-dependent effects on incident- and reflected-shock conditions over a
467 wide range of pressures and Mach numbers. *Combust Flame* 2020;217:200-211.
- 468 [25] Dayma G, Serinyel Z, Carbonnier M, Bai J, Zhu Y, Zhou CW, Kéromnès A, Lefort B,
469 Le Moyne L, Dagaut P. Oxidation of pentan-2-ol – part II: Experimental and modeling
470 study. *Proc Combust Inst* 2021;38:833-841.